Journal of Medicinal Chemistry

Article

pubs.acs.org/jmc

Development and *in Vivo* Quantitative Magnetic Resonance Imaging of Polymer Micelles Targeted to the Melanocortin 1 Receptor

Natalie M. Barkey,[†] Christian Preihs,[‡] Heather H. Cornnell,[†] Gary Martinez,[§] Adam Carie,[⊥] Josef Vagner,[∥] Liping Xu,[†] Mark C. Lloyd,[¶] Vincent M. Lynch,[‡] Victor J. Hruby,[▽] Jonathan L. Sessler,[‡] Kevin N. Sill,[⊥] Robert J. Gillies,[†] and David L. Morse*[,†]

[†]Department of Cancer Imaging and Metabolism, H. Lee Moffitt Cancer Center & Research Institute, Tampa, Florida, United States

[‡]Department of Chemistry and Biochemistry, University of Texas at Austin, Austin, Texas, United States

[§]Department of Small Animal Molecular Imaging, H. Lee Moffitt Cancer Center, Tampa, Florida, United States

[⊥]Intezyne Technologies, Inc., Tampa, Florida, United States

[∥]The BIO5 Research Institute, The University of Arizona, Tucson, Arizona, United States

[¶]Department of Analytic Microscopy, H. Lee Moffitt Cancer Center, Tampa, Florida, United States

[▽]Department of Chemistry & Biochemistry, The University of Arizona, Tucson, Arizona, United States

Supporting Information

ABSTRACT: Recent emphasis has focused on the development of rationally designed polymer-based micelle carriers for drug delivery. The current work tests the hypothesis that target specificity can be enhanced by micelles with cancer-specific ligands. In particular, we describe the synthesis and characterization of a new gadolinium texaphyrin (Gd-Tx) complex encapsulated in an IVECT micellar system, stabilized through Fe(III) cross-linking and targeted with multiple copies of a specific ligand for the melanocortin 1 receptor (MC1R), which has been evaluated as a cell-surface marker for melanoma. On the basis of comparative MRI experiments, we have been able to demonstrate that these Gd-Tx micelles are able to target MC1R-expressing xenograft tumors *in vitro* and *in vivo* more effectively than various control systems, including untargeted or un-cross-linked Gd-Tx micelles. Taken in concert, the findings reported herein support the conclusion that appropriately designed micelles are able to deliver contrast agent payloads to tumors expressing the MC1R.

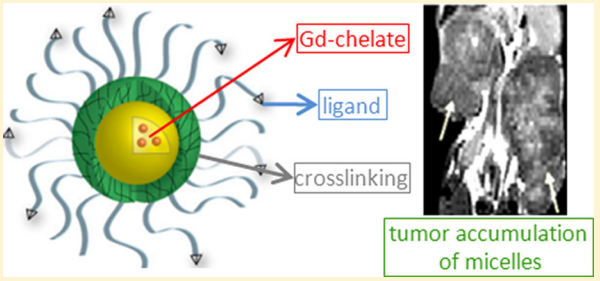

INTRODUCTION

Rationally designed, polymer-based micelle carriers represent a promising approach to the delivery of therapeutic or diagnostic payloads. They offer many potential advantages as delivery agents and could serve to (1) enhance the solubility of lipophilic drugs, (2) increase circulation times, and (3) lower the toxicity of the payload in question. Micelles with diameters between 20 and 200 nm are particularly attractive because particles of this size can escape renal clearance. This generally translates into longer circulation times and can lead to improved accumulation in tumor tissues as a result of the enhanced permeability and retention (EPR) effect.[1,2] It has also been suggested that selective accumulation in tumors relative to normal tissues can be enhanced through the use of tumor-specific cell-surface targeting groups and that binding events may be used to trigger release mechanisms. Such strategies are appealing since they could serve not only to enhance uptake in tumor relative to normal tissues but also to reduce toxicity in peripheral organs.[1−3]

Despite the advantages offered by micellar delivery systems, to date no micellar system has been described that achieves the full promise of targeting *in vivo*. Of additional concern is the fate of micelle delivery systems in biological media.[4] Previously described micelle delivery systems have suffered from an inherent instability *in vivo*, generally undergoing collapse in the presence of serum lipids and proteins.[4] Micelles can be stabilized for *in vivo* use through cross-linking of individual acyl chains. To date numerous cross-linking reactions have been attempted, employing strategies that range from the use of disulfides[5,6] and other redox-sensitive bonds[7] to temperature-[8] and pH-sensitive functional groups.[9−11] Here, we report a novel cross-linking procedure that relies on the pH sensitivity of metal−oxygen coordination bonds.[12] This particular form of cross-linking is known to increase blood circulation times and result in a stable micelle delivery system that is able to selectively dissociate and release its contents in acidic tumor microenvironments.[13]

There are a number of micelle-based delivery systems for drugs such as doxorubicin and paclitaxel currently in phase I

Received: January 4, 2013
Published: July 17, 2013

dx.doi.org/10.1021/jm4005576 | *J. Med. Chem.* 2013, 56, 6330−6338

Scheme 1. (A) Synthesis of Gadolinium−Texaphyrin (Gd-Tx) 1 and (B) Crystal Structure of 1 Obtained from Methanol[a]

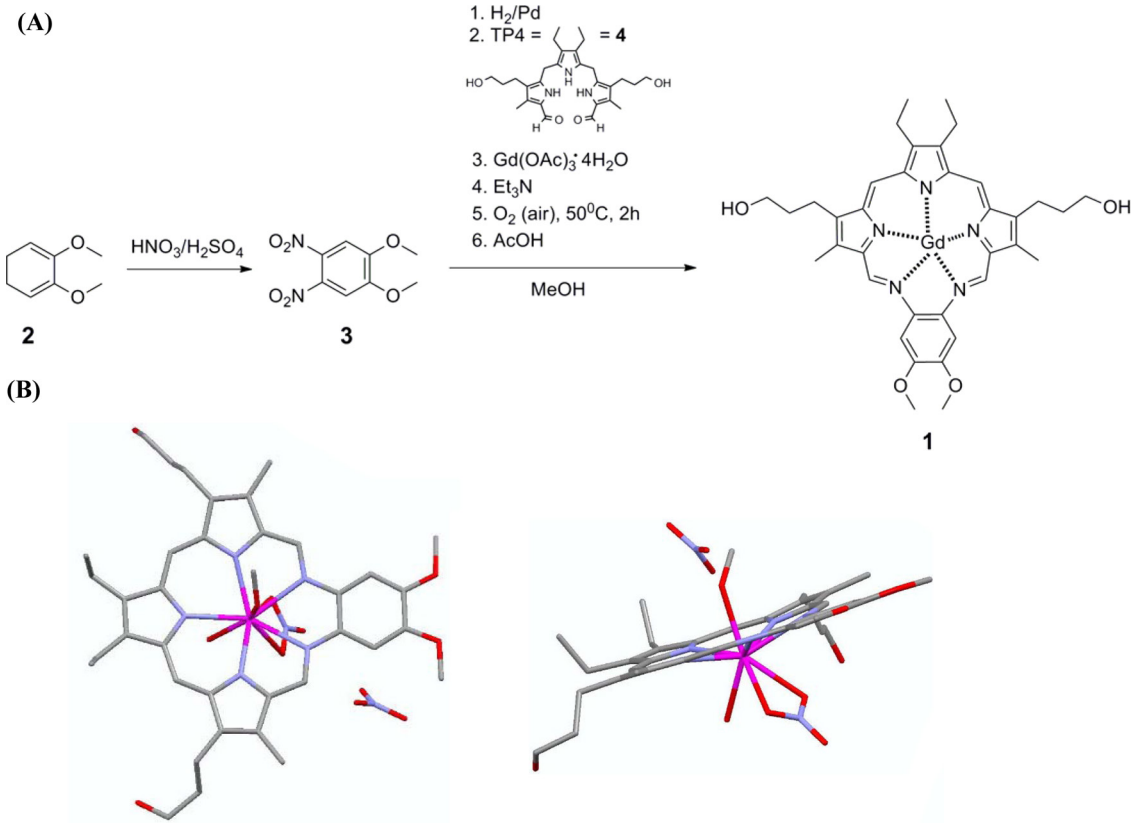

[a]Detailed information regarding the Gd-Tx crystal structure can be found in the Supporting Information.

and II clinical trials.[1,2] These systems provide for increased circulation times and larger area-under-the curve pharmacokinetics relative to the corresponding free drug. Some systems now in preclinical study are also "passively targeted,"[6,14,15] meaning they lack any specific surface ligands and rely solely on EPR to deliver their payload.[5,8,16] A significant disadvantage with passive targeting of micelle delivery systems is an increased probability for nonspecific delivery and accumulation in clearance organs, such as liver and kidney, relative to tumor.[2,17] Additionally, the significance of EPR in human cancers remains largely unproven and there is increasing evidence that EPR alone may not be enough to ensure the selective delivery of a payload.[17]

Most attempts at micelle targeting have come from the use of ligands such as $\alpha_v\beta_3$ (RGD), epidermal growth factor receptor (EGFR), or folate.[7,18−23] Unfortunately, most of these targeted systems suffer from a high peripheral toxicity,[5,7,16,19,20] have only seen limited testing *in vivo* (e.g., in animal models lacking tumor xenografts[21,22]), or have not yet quantitatively demonstrated selective tumor accumulation relative to peripheral organs.[7,11,18,23,24] It is also noteworthy that various other targeted systems have been reported to provide little improvement in tumor uptake compared with their untargeted controls.[7,19,20] Thus, there remains a need for more specific biological targeting agents, including those that rely on localization strategies that are not EPR dependent. This may be of particular relevance in clinical systems, where it has recently been proposed that human cancers have only a modest EPR compared with murine xenografts.[17]

One attractive target is the melanocortin 1 receptor (MC1R), which is expressed on over 80% of malignant melanomas.[25] Not surprisingly, the MC1R has been investigated as a target for delivery of imaging and therapeutic agents. Indeed, a number of MC1R ligands have been developed for this purpose.[26−29] The best known of these is based on the melanocyte stimulating hormone (MSH) structure, [Nle^4,DPhe^7]-α-MSH (NDP-α-MSH),[30] and is considered the "gold standard" for *in vitro* assays due to its ease of synthesis, low cost, and high MC1R affinity.[29,31] However, NDP-α-MSH is not selective for MC1R and displays strong nanomolar binding affinities to other melanocortin receptor isoforms, that is, MC3R, MC4R, and MC5R.[32−34] MC2R is not avid for MSH-based ligands.[35] MC3R and MC4R are primarily expressed in the human brain and CNS.[36−38] However, MC3R mRNA has been detected in human heart, and MC5R mRNA is expressed in human lung and kidney.[39] Expression in the brain is less of a concern because MSH-based targeted agents are not likely to cross the blood−brain barrier. Likewise, expression in the heart and lung is not likely to be problematic because, due to their mass, targeted micelles are expected to be restricted to the normal vasculature, although it is anticipated that they will enter tumors due to the permeable tumor vasculature (EPR effect). On the other hand, the expression of MC5R in the kidney is of concern due to kidney involvement in drug clearance, which could lead to off-target binding. Nevertheless it was expected that enhanced delivery to melanomas could be achieved through targeting the MC1R receptor. The present study was designed as an initial test of this hypothesis.

Koikov et al. has reported the development of a ligand, 4-phenylbutyryl-His-DPhe-Arg-Trp-NH_2, with high selectivity and specificity for MC1R.[28] We have recently altered this ligand with an alkyne (4-phenylbutyryl-His-DPhe-Arg-Trp-Gly-

dx.doi.org/10.1021/jm4005576 | J. Med. Chem. 2013, 56, 6330−6338

Scheme 2. Formulation of Gd-Tx Micelles

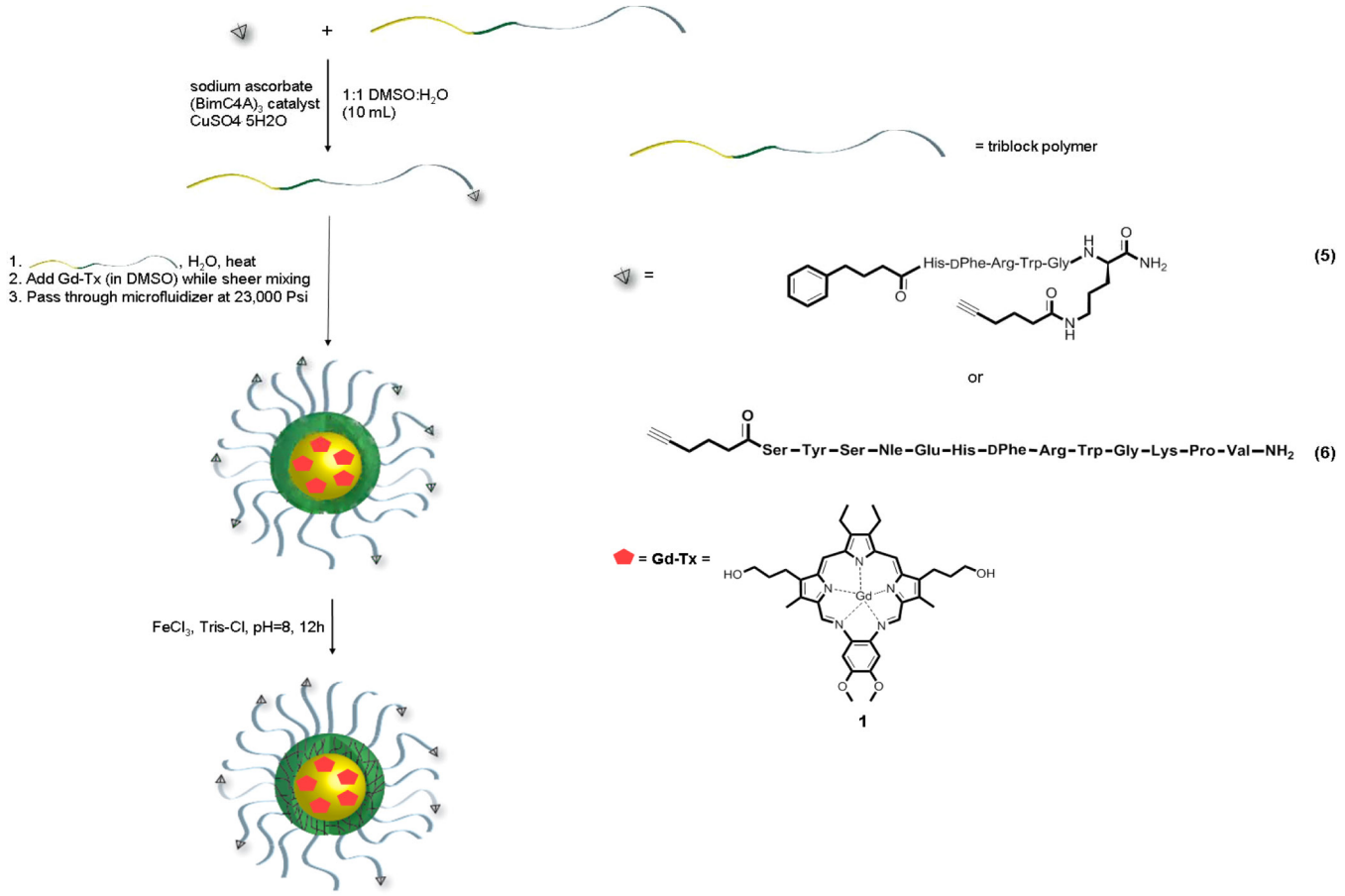

Lys(hex-5-ynoyl)-NH_2; **1**)[40] for click attachment to a micelle-forming triblock polymer. Moreover, we have demonstrated *in vitro* that micelles decorated with compound **1** retain the high binding affinity (2.9 nM K_i) of the free ligand and display improved target selectivity.[40] In this prior work, the K_i of targeted cross-linked (XL) micelles for MC1R was found be to four times lower than the corresponding targeted un-cross-linked (UXL) micelles while not binding to either of the undesired targets, MC4R or MC5R.[40] In this report, we show how these micelles can be used to deliver a contrast-enhancing agent.

Texaphyrins are a series of expanded porphyrins that have attracted interest in the area of cancer research.[41−44] Gadolinium complexes of texaphyrin (Gd-Tx) have been specifically evaluated in numerous clinical trials, including those for metastatic cancer to the brain, non-small-cell lung cancer (NSCLC) and non-Hodgkin's lymphoma.[43] The incorporation of gadolinium into the texaphyrin macrocycle allows the tissue distribution of Gd-Tx to be studied noninvasively via standard magnetic resonance imaging (MRI) methods.

To develop micelles containing Gd-Tx, we have taken advantage of a triblock polymer micelle system with enhanced stability (IVECT) that was initially developed by Intezyne Technologies Inc. (Tampa, FL).[13,40] This triblock polymer is composed of a hydrophobic encapsulation block, a responsive stabilizer block, and a hydrophilic masking block that contains an azide for functionalization via click chemistry. The main advantage of IVECT micelles over traditional micelles is the incorporation of the stabilization block, which allows the micelles to be cross-linked via a pH-sensitive Fe(III) metal coordination reaction.[12,13,40] They are also biodegradable and designed to release their payload in the acidic microenvironment of tumors.[13] As detailed below, this approach has allowed for the generation of a stabilized IVECT micelle system that incorporates Gd-Tx and that both penetrates into xenografted tumors with high selectively and clears from circulation without being retained in the kidney or liver. Tumor penetration, as inferred from MRI studies, was not observed with either untargeted or un-cross-linked micelles. On this basis, we suggest that the present approach provides for tumor-specific targeting that is superior to that provided by EPR alone.

RESULTS

Gadolinium−Texaphyrin (Gd-Tx) Structure. A single-crystal X-ray diffraction analysis of the Gd-Tx complex confirmed the expected planar structure for the core macrocycle and revealed several ancillary ligand and solvent interactions (Scheme 1).

Physical Properties of the Gd-Tx Micelles. The targeted Gd-Tx micelles were prepared using a novel optimized encapsulation strategy (Scheme 2). The average particle size was determined using standard dynamic light scattering (DLS, Particle Characterization Laboratories, Novato, CA) methods. The surface charge and gadolinium percent loading by weight were determined by ζ potential (Particle Characterization Laboratories) and elemental analyses (ICP-OES, Galbraith Laboratories, Knoxville, TN), respectively (Table 1). These

dx.doi.org/10.1021/jm4005576 | J. Med. Chem. 2013, 56, 6330−6338

Table 1. Summary of the Physical Properties of Gd-Tx Micelles

sample no.	stability[a]	targeting[b]	% Gd-Tx encap. (calcd)	% Gd-Tx encap. (actual)	charge (mV)	DLS size (nm)
1	UXL	UT	0.54	0.51	−17.70	88.90
2	UXL	T	0.53	0.50	−17.74	88.80
3	XL	UT	0.52	0.52	−10.73	87.50
4	XL	T	0.51	0.51	−9.49	82.50

[a]Micelles are stabilized with Fe(III) cross-linking (XL) reaction. UXL denotes un-cross-linked micelles. [b]Micelles are targeted (T) with an MC1R-specific ligand. UT denotes untargeted micelles.

studies provided support for the notion that there are no differences in micelle size for the cross-linked (XL) and un-cross-linked (UXL) pairs or for the targeted (T) and untargeted (UT) pairs. Particle charges ranged from −0.33 to −29 mV as deduced from ζ potential analyses.

Gd-Tx Micelle Stability. Cross-linked Gd-Tx micelles were dissolved in PBS at the critical micelle concentration (CMC, 0.02 mg/mL) and dialyzed for 6 h against PBS (pH 8 and pH 3). HPLC analyses of the Gd-Tx micelles pre- and postdialysis indicated that the cross-linked micelles retained >95% of the encapsulated Gd-Tx after dialysis at pH 8 and 50% of the encapsulated Gd-Tx at pH 3.

Competitive Binding Assays. Our established time-resolved lanthanide-fluorescence whole-cell competitive binding assays[33,40] were used to optimize ligand loading for maximal avidity. In these assays, increasing concentrations of micelles conjugated to the targeting ligand **6**, a version of NDP-α-MSH with an alkyne for attachment by click chemistry (Scheme 2), were measured for their ability to competitively displace Eu-labeled NDP-α-MSH. The remaining Eu was then measured using time-resolved fluorescence (TRF, see Materials and Methods). Because gadolinium(III) cations can potentially interfere with the lanthanide-based TRF binding assays,[33] unloaded triblock polymer micelles (i.e., free of Gd-Tx) targeted with 2.5% to 30% ligand **6** by weight loading (see Scheme 2) were used. Micelles stabilized with Fe(III) cross-linking (**6**-XL micelles) had the highest binding avidity at 5% ligand loading, as reflected in the lowest K_i (1.49 ± 0.12 nM K_i, n = 4, Figure 1). It was also observed that **6**-XL micelles had

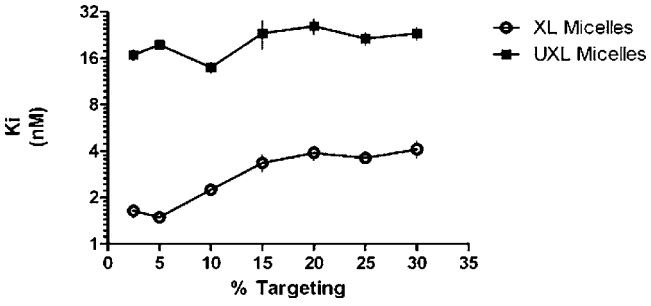

Figure 1. Effect of % ligand **6** coverage on micelle binding avidity.

significantly higher binding avidities at all ligand loading levels (p < 0.001). The same binding assays were also conducted with **5**-targeted XL and UXL micelles (5-XL and 5-UXL micelles, Scheme 2) at 5% ligand loading, as well as **5**-targeted monomeric polymer. Ligand **5** has greater specificity for MC1R relative to MC4R or MC5R isoforms, which are expressed in the kidney.[40] The K_i of the **5**-targeted XL micelles (2.9 ± 0.42 nM; n = 4) was 4 times lower than the corresponding UXL micelles (12 ± 2.6 nM; n = 4, Figure 1).[40] Control assays with untargeted micelles (UT-XL and UT-UXL) and untargeted monomeric polymer revealed no detectable interaction with the receptor.[40]

***In Vivo* MR Imaging.** SCID mice with subcutaneous MC1R-expressing tumors were injected with 0.5% w/w Gd-Tx micelles (T-XL, T-UXL, UT-XL, UT-UXL) via tail vein at a dose of 12 μmol Gd-Tx/kg. All targeted micelles used for *in vivo* imaging studies were formulated with 5% (w/w) of **5**-targeted polymer (**5**-UXL and **5**-XL). Using an Agilent 7T small animal MRI spectrometer, coronal T_1-weighted spin echo multislice (SEMS) images were acquired of each animal prior to and 1, 4, 12, 24, and 48 h after injection of the micelles. Following imaging, MC1R expression was confirmed in each tumor by immunohistochemistry staining (Supplemental Figure S4, Supporting Information). Figure 2 shows representative images of the center slices of the tumors of animals injected with the different 0.5% Gd-Tx loaded micelles recorded at different time-points.

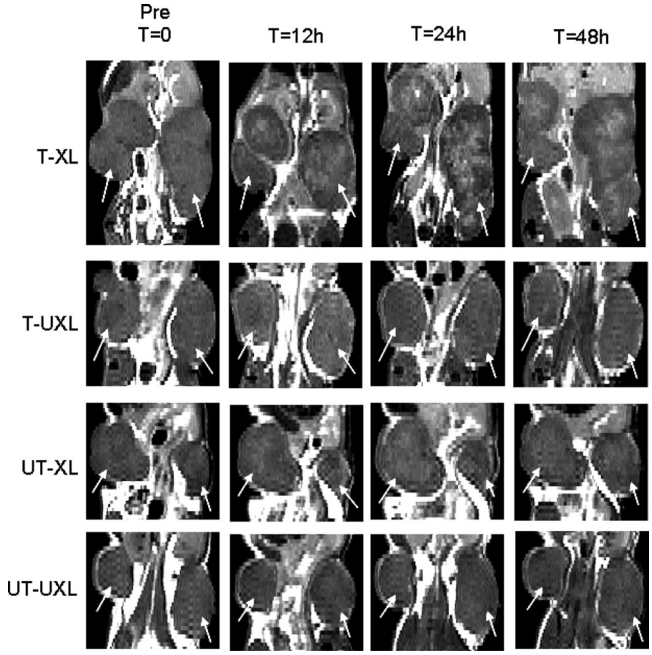

Figure 2. Coronal-90 T_1 weighted spin echo multislice (SEMS) images of mice treated with different Gd-Tx micelle formulations. Representative images from each group of mice treated with 0.5% Gd-Tx micelles at selected time points. White arrows denote location of tumors.

To quantify enhancement due to tumor uptake of the micelles, intensity histograms for right (R) and left (L) whole tumors, kidneys, and livers were prepared using a MATLAB program (Mathworks) by drawing a region of interest (ROI) across all applicable slices for each time point. A mean intensity value was then calculated and normalized to thigh muscle because contrast material is not expected to be present in the muscle (see Materials and Methods). Figure 3 shows the percent change in intensity from pre- to postinjection in tumors (a, b), kidneys (c), and liver (c) for each 0.5% Gd-Tx micelle group over a 48 h time course (for full clearance data, see Figure S5, Supporting Information). By one-way ANOVA with Tukey's multiple comparison test, the **5**-XL micelle group had a

dx.doi.org/10.1021/jm4005576 | J. Med. Chem. 2013, 56, 6330−6338

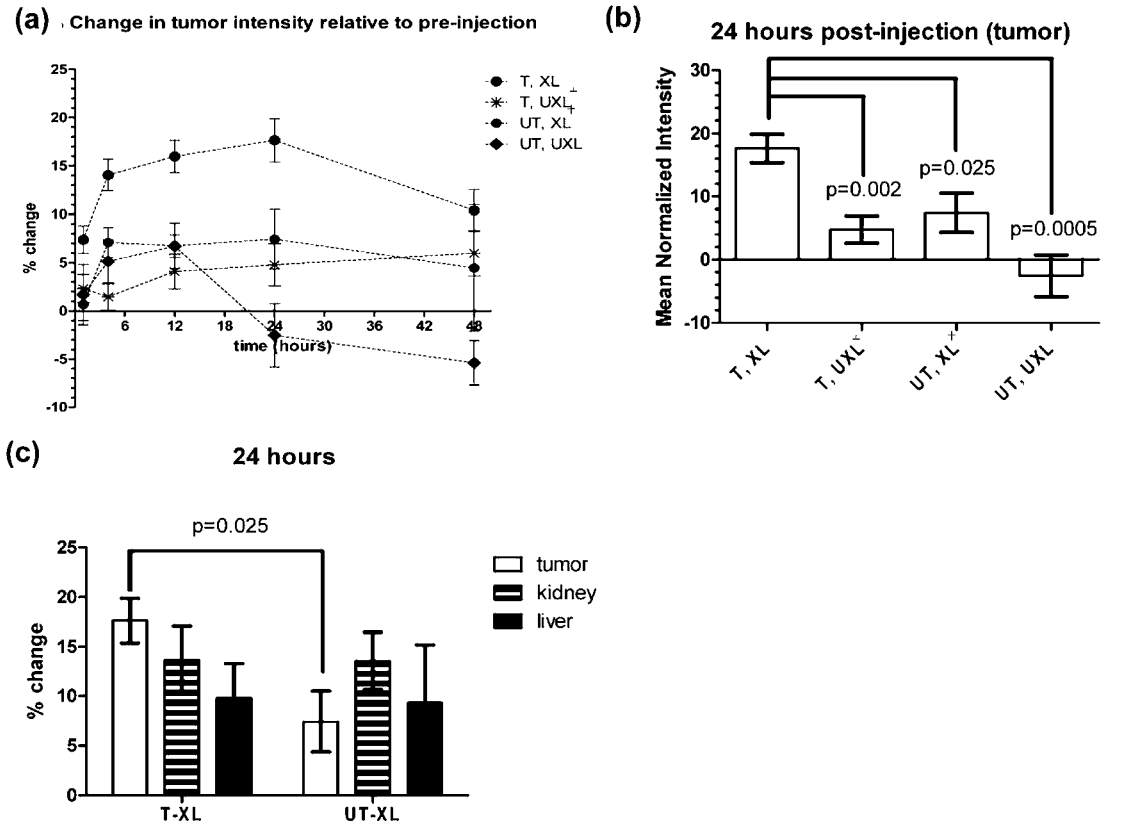

Figure 3. Buildup and clearance data of Gd-Tx contrast enhancement in (a, b) tumor and (c) tumor, liver, and kidney (24 h). *p*-values are in comparison to T-XL group. All groups contained three mice except where noted. [⊥]One mouse expired between 24 and 48 h time point. [†]One mouse expired upon injection of micelle agent.

significantly higher change in contrast enhancement in the tumors relative to the other groups at all time points, $p < 0.05$ (**3a**), with a peak accumulation occurring at 24 h (**3b**). The increased enhancement in the tumors of animals injected with the 0.5% Gd-Tx **5**-XL micelles can be visualized in the postinjection MR images (Figure 2, top row) relative to tumors in all other animals injected with the control formulation (UT-XL, **5**-UXL, UT-UXL). Again, no other micelle group displayed visible tumor uptake.

By one-way ANOVA with Tukey's multiple comparison test, both groups with cross-linked micelles (XL) had a significantly higher change in contrast pre- to postinjection in the kidneys compared with the UXL groups, but there was no significant difference when the **5**-XL and UT-XL or the T-UXL and UT-UXL time courses were compared. Contrast enhancement for the XL micelles peaked in the kidneys ∼1−4 h. There was no significant difference in enhancement in the liver among the different time courses.

DISCUSSION

Europium time-resolved fluorescence (TRF) whole-cell competition binding assays conducted with both **5**- and **6**-targeted micelles provide support for the central hypothesis underlying this study, namely, that cross-linking provides stability to the micelle system and that the composition of the micelle can be modified to allow for targeting. Eu-NDP-α-MSH was chosen as a model ligand for competition due to its relatively high affinity for MC1R (1.9 nM) and for the ease of synthesis that it provides.[29,31] In the percent targeting optimization assays with an alkyne-functionalized NDP-α-MSH (**6**, Scheme 2), there was a clear difference between the binding affinities of the cross-linked (**6**-XL) and un-cross-linked (**6**-UXL) micelles (Figure 1). This finding is ascribed to the Fe(III) cross-linking, which serves to stabilize the micelles in biological media. In the absence of cross-linking, the micelles dissociate, in whole or in part, to free monomers, leading to a loss of structural integrity and the premature release of the payload (the encapsulated contrast agent in the present instance). A second advantage of cross-linking is that it leads to an operational increase in binding avidity, a result that may reflect a benefit of multivalent interactions. The **5**-targeted (T) micelles of this study also exhibited a stronger avidity to the MC1R receptor when cross-linked (**5**-XL) compared with their un-cross-linked counterpart (T-UXL), a finding we take as further support for the contention that (i) cross-linking stabilizes micelles and (ii) multiple ligands on the micelle surface provide for enhanced binding.

The above Gd-Tx containing micelles (0.5% Gd-Tx w/w) were further studied *in vivo*. In accord with the design expectations, these *in vivo* experiments revealed improved MRI contrast enhancements upon administration of the Gd-Tx containing **5**-XL micelles, with maximal enhancement observed at 24 h. As can be seen by an inspection of Figures 2 and 3, this enhancement was not seen with the other micelle systems, supporting the contention that the **5**-XL micelles provide good systems for effecting tumor localization and payload delivery. The maximum enhancement was 17% compared with preinjection images. While this enhancement is likely not large enough to be clinically valid for imaging in the current formulation, it is encouraging that similar stabilized micelle

dx.doi.org/10.1021/jm4005576 | J. Med. Chem. 2013, 56, 6330−6338

formulations have demonstrated significant tumor uptake of therapeutic payload and increased therapeutic efficacy relative to untargeted drug administration.[13,45] The results of this study thus provide support for the contention that targeted formulations can provide for improvements in efficacy through increased delivery of payload throughout the tumor.

Although the *in vivo* studies were conducted using a colorectal cancer cell line (HCT116) engineered to express MC1R at a level of 240 000 receptors per cell,[46] we have recently conducted *in vivo* studies using the same MC1R targeting ligand (**5**) conjugated to a near-infrared fluorescent dye and using melanoma tumor lines with high (B16) and low (A375) endogenous expression of MC1R.[47] Blocking studies demonstrated specific uptake of the labeled ligand into tumors bearing these melanoma cells and uptake was correlated with MC1R expression levels. To demonstrate clinical relevance, additional work will be needed that, inter alia, demonstrates uptake of ligand **5** targeted micelles into tumor xenografts containing melanoma cells with lower endogenous MC1R expression levels. However, these future studies lie outside the scope of the present proof-of-principle analyses.

The unique ability of the **5**-XL micelles to penetrate the tumor appears to result from a combination of the MC1R-specific targeting group and the enhanced stability provided by the Fe(III) cross-linking. If targeting alone were enough to produce effective tumor enhancement, we would also observe a substantial uptake in the case of the **5**-UXL micelles. Likewise, if cross-linking and EPR alone were enough to effect accumulation, we would observe an increased build-up in the UT-XL group. Finally, it is important to note that the enhancement observed in the **5**-XL group was not the result of free Gd-Tx (which is known to accumulate in tumors selectively[42,43,48,49]). If this were the case, we would have observed enhanced uptake in all four micelle groups (i.e., UT-UXL, **5**-UXL, and UT-UXL, in addition to the **5**-XL system). This was not seen; thus, the *in vivo* data are consistent with the conclusion that the Gd-Tx containing **5**-XL micelles allow for functionally acceptable binding avidity, stability, tumor penetration, and uptake. Presumably, the cross-linking reaction stabilizes the micelles after administration and during initial time points while they circulate throughout the bloodstream, while the targeting group allows the system to bind to and be retained within the tumor cells. Interestingly, the XL micelle groups had significantly elevated enhancement in the kidneys relative to the UXL groups, although this uptake was nonspecific. This may be a result of the increased stability of the XL micelles resulting in longer circulation times and slower rates of complete clearance through the renal system into the bladder. Also, the timing of kidney clearance of the XL micelles is comparable in timing to near-infrared fluorescent dye conjugates to monoclonal antibodies with comparable mass.[50]

We have previously reported the development of a ligand specific to MC1R, and we have shown that the conjugation of this ligand to the IVECT micelle system does not result in a significant decrease in binding avidity.[40] In this report, we describe the synthesis, incorporation, and characterization of a new gadolinium texaphyrin (Gd-Tx) that is characterized by a high inherent T_1 relaxivity. We also detail its encapsulation within the IVECT system and the production of cross-linked micelles by reaction with Fe(III). Moreover, we have demonstrated that the targeted Gd-Tx micelles are selectively retained in target-expressing xenograft tumors *in vivo*. As expected, MRI contrast enhancement was not visually observed within the heart, lung, brain, or CNS following clearance from vascular circulation. While nonspecific uptake into the kidney and liver was observed, targeted micelles were not specifically retained in the kidney relative to untargeted, which suggests only nonspecific clearance as opposed to off-target uptake in these organs. To the best of our knowledge, this is the first example of a targeted micelle that is capable of carrying a payload and that outperforms systems based on EPR in terms of tumor penetration, uptake, and retention.

Advantages of the current system include the following: (1) the target, MC1R, is highly expressed in melanoma cells and not in healthy tissues, except for melanocytes; (2) the system demonstrates high short-term stability, and (3) it demonstrates an ability to specifically accumulate in tumors, compared with nonspecific uptake in clearance organs. These attributes are reflected in the *in vivo* images that reveal uptake of targeted constructs relative to untargeted deep within the tumor with peak accumulation at 24 h. In contrast, peak nonspecific accumulation in the kidney and liver was seen at 1−4 h. These differences are thought to reflect the benefits of targeting. However, biodegradation of the stabilized micelles may also contribute to the effect; to the extent it occurs on short time scales (on the order of hours), it would allow for release of payload (Gd-Tx) within the tumor while concurrently clearing from circulation. While further investigations will be required to detail the full pharmacokinetic profile of these new micelles and to develop formulations that deliver more clinically relevant payloads, it is important to appreciate that from an operational perspective the systems of this report constitute the first example of targeted micellar constructs that are capable of delivering payloads in a tumor selective fashion.

MATERIALS AND METHODS

Synthesis of Gd-Tx. All chemicals were obtained from commercial sources (Fisher Scientific, Acros Chemicals, Sigma-Aldrich or Strem Chemicals) and used as supplied unless otherwise noted. All solvents were of reagent grade quality. Fisher silica gel (230−400 mesh, grade 60 Å) and Sorbent Technologies alumina (neutral, standard activity I, 50−200 μm) were used for column chromatography. Thin layer chromatography (TLC) analyses were performed on silica gel (aluminum backed, 200 μm or glass backed, 250 μm) or alumina neutral TLC plates (polyester backed, 200 μm), both obtained from Sorbent Technologies. Low- and high-resolution ESI mass spectra (MS) were obtained at the Mass Spectrometry Facility at The University of Texas at Austin using a Thermo Finnigan LTQ instrument and an Qq FTICR (7 T) instrument, respectively. HPLC spectra were taken on a Shimadzu high performance liquid chromatograph (fraction collector module FRC-10A, autosampler SIL-20A, system controller CBM-20A, UV/vis photodiode array detector SPD-M20A, Prominence). The tripyrrane dialdehyde species **4** (generally referred to as "TP-4") was provided by Pharmacyclics Inc. and synthesized as previously described.[49] The precursor 1,2-dimethoxy-4,5-dinitrobenzene **3** was synthesized as previously described.[51]

The gadolinium complex used in this study (Gd-Tx, **1**) was prepared as shown in Scheme 1. Briefly, compound **3** (1 g, 4.38 mmol) was dissolved in 10 mL of methanol and placed in a hydrogenation flask. The solution was purged with nitrogen for 5 min, and palladium on activated carbon (10%, 0.1 g) was added. The mixture was degassed and allowed to react with hydrogen gas at 100 psi with agitation for 18 h, filtered under Schlenk conditions through a minimal pad of Celite, and added instantly to a solution of TP-4, **4** (2.11 g, 4.38 mmol), in 15 mL of methanol under nitrogen at 70 °C. Aqueous hydrochloric acid was added (2 mL, 0.5 M), and the deep red reaction mixture was stirred for 4 h. Next, gadolinium acetate tetrahydrate (2.67 g, 6.57 mmol, 1.5 equiv) was added together with 3 mL of triethylamine, and

dx.doi.org/10.1021/jm4005576 | J. Med. Chem. 2013, 56, 6330−6338

the solution was stirred at 70 °C for 16 h, during which time the solution gradually changed color from deep red to deep green. The solvent was removed *in vacuo*, and the residue was subjected to column chromatography (silica gel). To remove apolar impurities, the column was eluted with a mixture of 95% CH_2Cl_2 and 5% MeOH. The product slowly starts to elute when a mixture of 60% CH_2Cl_2 and 40% MeOH is used as the eluent. The deep green fraction isolated using this eluent mixture was collected, and the solvent was removed *in vacuo* to give **1** (Gd-Tx) as a deep green crystalline material (1.63 g, 42%). UV/vis (MeOH, 25 °C): λ_{max} =470 (Soret-type band); 739 (Q-type band). Low resolution MS (ESI in MeOH): 797.25 ($M^+ - 2OAc$ + OMe), 825.42 ($M^+ - OAc$). High resolution MS (ESI in MeOH): calculated for $[C_{38}H_{45}N_5O_6Gd^{+1}]^+$ = 825.2611; found 825.2621 ($[C_{38}H_{45}N_5O_6Gd^{+1}]^+$; $M^+ - OAc$). The Gd-Tx **1** samples used in the present study were confirmed as 99.5% pure by HPLC. Additional data, including mass spectra and HPLC traces for Gd-Tx **1** can be found in the Supporting Information.

Crystallization of Gd-Tx and Determination of Structure. Crystals suitable for X-ray diffraction were obtained by dissolving Gd-Tx **1** (2 mg, 2.26 μmol) in 1 mL of methanol. Sodium nitrate (0.2 mg, 4 equiv.) was added, and the solution was heated to reflux at 60 °C for 24 h. At this point, 0.25 mL of chloroform was added, the solution was placed in a vial, and diethyl ether was allowed to slowly diffuse into the solution at 5 °C. For full crystallographic data, see Supporting Information. Further details of the structure may also be obtained from the Cambridge Crystallographic Data Centre by quoting CCDC number 859294.

Synthesis of Targeted Triblock Polymers. IVECT triblock polymers with a terminal azide were obtained from Intezyne Technologies (Tampa, FL), and either **5**[40] or **6** was synthesized (Scheme 2) and analyzed for purity (>95%) by analytical HPLC and MS by ESI or MALDI-TOF and used as the MC1R-selective ligand. Standard click chemistry was conducted as previously published.[40] Unconjugated polymer was characterized by NMR and GPC analysis, which showed a single, monomodal peak. The polymer conjugated to the MC1R-selective ligand was determined by NMR to be >95% pure.

Formulation and Stabilization of Gd-Tx Micelles. For targeted formulations, a percentage (5% in most cases) of the targeted polymer was used, and the remainder (95% in most cases) was made up of untargeted polymer. The triblock polymer (750 mg) was dissolved in water (150 mL) at a concentration of 5 mg/mL and stirred with slight heating until fully dissolved. After cooling to room temperature, the polymer solution was placed in a sheer mixer, and the Gd-Tx **1** solution (0.5% w/w in 380 μL of dimethyl sulfoxide) was added. The resulting solution was then passed through a microfluidizer (Microfluidics M-110Y) at 23 000 PSI, filtered through a 0.22 μm Steriflip-GP filter unit (Millipore), and lyophilized.

For stabilized formulations, micelles were subject to an Fe(III)-mediated cross-linking reaction.[12] $FeCl_3$ was prepared at concentration of 1.35 g/mL in 20 mM Tris-Cl (pH 7.4). The targeted and untargeted micelles were then dissolved in the Fe(III)-Tris solution at a concentration of 20 mg/mL, and the solution was adjusted to pH 8 through the dropwise addition of 0.1−1.0 M aqueous NaOH. The cross-linking reaction was stirred for 12 h, and the contents of the reaction vessel were then lyophilized.

Cell Culture. HCT116 cells overexpressing hMC1R were engineered in our laboratory. HCT116 cells were transfected with the pCMV6-Entry Vector (Origene; RC 203218) using the Fugene 6 transfection reagent (Roche; 1814-443). Transfected cells were grown in a selection media containing 0.4 mg/mL Geneticin (Life Technologies; 11811-031) and tested for the hMC1R cell surface expression by saturation binding assay.[23] Cells were maintained under standard conditions (37 °C and 5% CO_2) and were grown in Dulbecco's modified Eagle medium (DMEM) supplemented with 10% FBS and 5% penicillin/streptomycin. Geneticin (G418S, 0.8%) was added to the media to ensure proper selection. hMC1R expression was verified through immunohistochemistry (IHC, see Supporting Information).

Europium Binding Assays. Our established europium lanthanide time-resolved fluorescence whole-cell saturation and competitive binding assays were conducted as previously published using the HCT116 cells engineered to express MC1R and the Eu-NDP-α-MSH ligand, which has known binding affinity for MC1R.[33,40]

***In Vivo* Murine Tumor Models.** All animal experiments were conducted under a protocol approved by the University of South Florida Institutional Animal Care and Use Committee (IACUC). These experiments adhere to the guidelines on the care and use of animals in research. HCT116/hMC1R-expressing flank tumor xenograft models were studied in female SCID/beige mice obtained from Harlan Laboratories at 6−8 weeks of age. HCT116/hMC1R cells were injected at concentrations of (3−10) × 10^6 cells per 0.1 mL of phosphate-buffered saline. Tumor volume measurements were made biweekly and calculated by multiplying the length by the width squared and dividing by two. Final volume measurements were determined through ROI analysis on the MRI, and all tumors imaged ranged from 300 to 500 mm^3 in volume.

MRI Imaging and Analysis. All imaging was completed on a 7 T, 30 cm horizontal bore Agilent magnetic resonance imaging (MRI) spectrometer ASR310 (Agilent Life Sciences Technologies, Santa Clara, CA). Once the tumors in the animals reached an average of ∼500 mm^3, the animals were pair-matched by tumor size and sorted into four groups to receive the following micelles: **5**-XL, UT-XL, **5**-UXL, or UT-UXL. Each animal was imaged the day before micelle injection for "pre" images. The following morning, each animal was individually administered 12 μmol/kg Gd-Tx (as Gd-Tx micelles) dissolved in 200 μL of saline via tail vein injection, and the time of injection was noted. Follow-up MRI images were taken at 1, 4, 12, 24, and 48 h postinjection of the micelles.

All animals were sedated using isoflurane and remained under anesthesia for the duration of the imaging. Animals were kept at body temperature (∼37 °C) using a warm air blower; the temperature of the air was adjusted to maintain the body temperature and was monitored using a fiber optic rectal probe. SCOUT images were taken to determine animal position within the magnet and setup the slices for the T_1 weighted spin echo multislice (SEMS) images. The SEMS images were taken as coronal-90 images (read direction along the *X*-axis, phase-encode along the *Z*-axis), with data matrix of 128 × 128 and a FOV of 40 mm (read) × 90 mm (phase); 15 1-mm thick slices were taken with a 0.5 mm gap between slices; the TR was 180 ms, and TE was 8.62 ms; there were eight averages taken for each image, resulting in a total scan time of about 3 min per SEMS image.

Images were processed using MATLAB (Mathworks, Natick, MA) to draw regions of interest (ROI) in the tumors, kidney, liver, and thigh muscle over multiple slices for each mouse at each time point. All intensities for each area of interest were averaged to determine a mean intensity. The mean intensity of each area was then normalized to the mean intensity of the thigh to generate a normalized intensity (NI):

$$\mathrm{NI} = \frac{I_{\mathrm{tumor}}}{I_{\mathrm{thigh}}}$$

A percent change value was then calculated by comparing each normalized time point after injection to the normalized preinjection intensity mean:

$$\%\mathrm{change} = \frac{\mathrm{NI}_{12h}}{\mathrm{NI}_{\mathrm{pre}}} \times 100$$

Since the right and left tumors are histologically equivalent (Figure S4, Supporting Information), the % change values for all tumors were averaged to obtain an "average tumor % change" at time points 1−24 h. Percent change values were also averaged for R and L kidney to obtain an "average kidney % change" at time points 1−24 h.

■ ASSOCIATED CONTENT

Ⓢ Supporting Information

Analytic spectra for compound, immunohistochemical staining of xenograft tumors for MC1R expression, a quantified time course of liver, kidney, and tumor clearance, *in vitro* phantom imaging data, and X-ray crystallography data for compound **1**.

This material is available free of charge via the Internet at http://pubs.acs.org.

AUTHOR INFORMATION

Corresponding Author

*Mailing address: H. Lee Moffitt Cancer Center & Research Institute, Department of Cancer Imaging and Metabolism, 12902 Magnolia Dr., SRB4, Tampa, FL 33612. Phone: 813-745-8948. E-mail: David.Morse@moffitt.org.

Author Contributions

All authors contributed to the writing of this manuscript.

Notes

The authors declare no competing financial interest.

ACKNOWLEDGMENTS

Research was funded by the Bankhead Coley Melanoma Pre-SPORE Program (Grant 02-15066-10-03) to D.L.M., NIH/NCI (Grant R01 CA 097360 to R.J.G. and D.L.M.; CA 68682 to J.L.S.), and Intezyne Inc. (Award No. 84-16301-01-01) to R.J.G. for a portion of N.M.B.'s salary and polymer materials. The authors acknowledge Professor Dean Sherry (UTSW) for his invaluable wisdom and insight.

ABBREVIATIONS USED

IVECT, Trademarked name of Intezyne Technology's triblock polymer; Gd-Tx, gadolinium texaphyrin; RGD, integrin $\alpha_v\beta_3$ three amino-acid residue ligand (arginine, glycine, aspartic acid); MC1R, melanocortin 1 receptor; MSH, melanocyte stimulation hormone; MC3R, melanocortin 3 receptor; MC4R, melanocortin 4 receptor; MC5R, melanocortin 5 receptor; MC2R, melanocortin 2 receptor; XL, cross-linked; UXL, uncross-linked; T, targeted; UT, untargeted; TRF, time-resolved fluorescence; SEMS, spin echo multislice; R, right; L, left; ROI, region of interest; IACUC, institutional animal care and use committee

REFERENCES

(1) Yokoyama, M. Clinical Applications of Polymeric Micelle Carrier Systems in Chemotherapy and Image Diagnosis of Solid Tumors. *J Exp Clin Med* **2011**, *3*, 151−158.

(2) Oerlemans, C.; Bult, W.; Bos, M.; Storm, G.; Nijsen, J. F. W.; Hennink, W. E. Polymeric micelles in Anticancer Therapy: Targeting, Imaging, and Triggered Release. *Pharm. Res.* **2010**, *27*, 2569−2589.

(3) Kedar, U.; Phutane, P.; Shidhaye, S.; Kadam, V. Advances in Polymeric Micelles for Drug Delivery and Tumor Targeting. *Nanomedicine* **2010**, *6*, 714−729.

(4) Kim, S.; Shi, Y.; Kim, J. Y.; K., P.; Chen, J.-X. Overcoming the barriers in micellar drug delivery: Loading efficiency, in vivo stability, and micelle−cell interaction. *Expert Opin. Drug Delivery* **2010**, *7*, 49−62.

(5) Shiraishi, K.; Kawano, K.; Maitani, Y.; Yokoyama, M. Polyion Complex Micele MRI Contrast Agents from Poly (ethylene glycol)-b-poly(L-lysine) Block Copolymers having Gd-DOTA; Preparations and their Control of T1 Relaxitivities and Blood Circulation Characteristics. *J. Controlled Release* **2010**, 1−8.

(6) Li, J.; Huo, M.; Wang, J.; Zhou, J.; Mohammas, J.; Zhang, Y.; Zhu, Q.; Waddad, A.; Zhang, Q. Redox-sensitive micelles self-assembled from amphiphilic hyaluronic acid-deoxycholic acid conjugates for targeted intracellular delivery of paclitaxel. *Biomaterials* **2012**, *33*, 2310−2320.

(7) Lee, H.; Hoang, B.; Fonge, H.; Reilly, R.; Allen, C. In-Vivo Distribution of Polymeric Nanoparticles at the Whole Body, Tumor and Cellular Levels. *Pharm. Res.* **2010**, *27*, 2343−2355.

(8) Kim, T.; Chen, Y.; Mount, C.; Gambotz, W.; Li, X.; Pun, S. Evaluation of Temperture-Sensitive, Indocyanine Green-Encapsulating Micelles for Noninvasive Near-Infrared Tumor Imaging. *Pharm. Res.* **2010**, *27*, 1900−1913.

(9) Jia, Z.; Wong, L.; Davis, T. P.; Bulmus, V. One-pot conversion of RAFT-generated multifunctional block copolymers of HPMA to doxorubicin conjugated acid- and reductant-sensitive crosslinked micelles. *Biomacromolecules* **2008**, *9*, 3106−3113.

(10) Yang, X.; Grailer, J. J.; Pilla, S.; Steebe, D. A.; Gong, S. Tumor-Targeting, pH-Responsive, and Stable Unimolecular Micelles as Drug Nanocarriers for Targeted Cancer Therapy. *Bioconjugate Chem.* **2010**, *21*, 496−504.

(11) Li, Y.; Xio, W.; Xiao, K.; Berti, L.; Luo, J.; Tseng, H.; Fung, G.; Lam, K. Well-definied reversible boronate crosslinked nanocarriers for targeted drug delivery in response to acidic pH values and cis-diols. *Angew. Chem., Int. Ed.* **2012**, *51*, 1−7.

(12) Cannan, R. K.; Kibrick, A. Complex Formation between Carboxylic Acids and Divalent Metal Cations. *J. Am. Chem. Soc.* **1938**, *60*, 2314−2320.

(13) Rios-Doria, J.; Carie, A.; Costich, T.; Burke, B.; Skaff, H.; Panicucci, R.; Sill, K. A versatile polymer micelle drug delivery system for encapsulation and in vivo stabilization of hydrophobic anticancer drugs. *J. Drug Delivery* **2012**, No. 951741.

(14) Sun, T.-M.; Du, J.-Z.; Yao, Y.-D.; Mao, C.-Q.; Dou, S.; Huang, S.-Y.; Zhang, P.-Z.; Leong, K.; Song, E.-W.; Wang, J. Simultaneous delivery of siRNA and pacilitaxel via a "two-in-one" micelleplex promotes synergistic tumor supression. *ACS Nano* **2011**, *5*, 1483−1494.

(15) Koo, H.; Huh, M.; Sun, I.-C.; Yuk, S.; Choi, K.; Kim, K.; Kwon, I. In vivo targeted delivery of nanoparticles for theranosis. *Acc. Chem. Res.* **2011**, *44*, 1018−1028.

(16) Tang, N.; Dy, G.; Wang, N.; Liu, C.; Hang, H.; Liang, W. Improving Penetration in Tumors with Nanoassemblies of Phospholipids and Doxorubicin. *J. Natl. Cancer Inst.* **2007**, *99*, 1004−1015.

(17) Chrastina, A.; Massey, K. A.; Schnitzer, J. E. Overcoming in vivo barriers to targeted nanodelivery. *Wiley Interdiscip. Rev.: Nanomed. Nanobiotechnol.* **2011**, *3*, 421−437.

(18) Kessinger, C.; Khemtong, C.; Togao, O.; Takahashi, M.; Sumer, B.; Gao, J. In-vivo angiogenesis imaging of solid tumors by avb3-targeted, dual-modality micellar nanoprobes. *Exp. Biol. Med.* **2010**, *235*, 957−965.

(19) Poon, Z.; Lee, J.; Huang, S.; Prevost, R.; Hammond, P. Highly Stable, Ligand Clustered "Patchy" Micelle Nanocarriers for Systemic Tumor Targeting. *Nanomedicine* **2010**, 1−30.

(20) Lee, H.; Fonge, H.; Hoang, B.; Reilly, R.; Allen, C. The Effects of Particle Size and Molecular Targeting on teh Intratumoral and Suncellular Distribution of Polymeric Nanoparticles. *Mol. Pharmaceutics* **2010**, *7*, 1195−1208.

(21) Hu, J.; Qian, Y.; Wang, X.; Liu, W.; Liu, S. Drug-Loaded and Superparamagnetic Iron Oxide Nanoparticle Surface-Embedded Amphiphilic Block Copolymer Micelles for Integrated Chemotherapeutic Drug Delivery and MR Imaging. *Langmuir* **2012**, *28*, 2073−2082.

(22) Liu, T.; Liu, X.; Qian, Y.; Hu, X.; Liu, S. Multifunctional pH-Disintegrable micelle nanoparticles of asymmetrically functionalized beta-cyclodextrin-based star copolymer covalently conjugated with doxorubicin and DOTA-Gd moieties. *Biomaterials* **2012**, *33*, 2521−2531.

(23) Xiong, X.-B.; Lavasanifar, A. Traceable Multifunctional Micellar nanocarriers for Cancer-Targeted Co-delivery of MDR-1 siRNA and Doxorubicin. *ACS Nano* **2011**, *5*, 5202−5213.

(24) Yang, R.; Meng, F.; Ma, S.; Huang, F.; Liu, H.; Zhong, Z. Galactose-decorated cross-linked biodegradable poly9ethylene glycol)-b-poly(E-caprolactone) block copolymer micelles for enhanced hepatoma-targeting delivery of paclitaxel. *Biomacromolecules* **2011**, *12*, 3047−3055.

(25) Siegrist, W.; Solca, F.; Stutz, S.; Giuffre, L.; Carrel, S.; Girard, J.; Eberle, A. N. Characterization of receptors for alpha-melanocyte-

stimulating hormone on human melanoma cells. *Cancer Res.* **1989**, *49*, 6352−6358.
(26) Cai, M.; Varga, E. V.; Stankova, M.; Mayorov, A.; Perry, J. W.; Yamamura, H. I.; Trivedi, D.; Hruby, V. J. Cell signaling and trafficking of human melanocortin receptors in real time using two-photon fluorescence and confocal laser microscopy: differentiation of agonists and antagonists. *Chem. Biol. Drug Des.* **2006**, *68*, 183−193.
(27) Mayorov, A. V.; Han, S. Y.; Cai, M.; Hammer, M. R.; Trivedi, D.; Hruby, V. J. Effects of macrocycle size and rigidity on melanocortin receptor-1 and −5 selectivity in cyclic lactam alpha-melanocyte-stimulating hormone analogs. *Chem. Biol. Drug Des.* **2006**, *67*, 329−335.
(28) Koikov, L. N.; Ebetino, F. H.; Solinsky, M. G.; Cross-Doersen, D.; Knittel, J. J. Sub-nanomolar hMC1R agonists by end-capping of the melanocortin tetrapeptide His-D-Phe-Arg-Trp-NH(2). *Bioorg. Med. Chem. Lett.* **2003**, *13*, 2647−2650.
(29) Chen, J.; Giblin, M. F.; Wang, N.; Jurisson, S. S.; Quinn, T. P. In vivo evaluation of 99mTc/188Re-labeled linear alpha-melanocyte stimulating hormone analogs for specific melanoma targeting. *Nucl. Med. Biol.* **1999**, *26*, 687−693.
(30) Sawyer, T.; Sanfilippo, P.; Hruby, V.; Engel, M.; Heward, C.; Burnett, J.; Hadley, M. 4-Norleucine, 7-D-phenylalanine-alpha-melanocyte-stimulating hormone: A highly potent alpha-melanotropin with ultralong biological activity. *Proc. Natl. Acad. Sci. U. S. A.* **1980**, *77*, 5754−5758.
(31) Chen, J.; Cheng, Z.; Hoffman, T. J.; Jurisson, S. S.; Quinn, T. P. Melanoma-targeting properties of (99m)technetium-labeled cyclic alpha-melanocyte-stimulating hormone peptide analogues. *Cancer Res.* **2000**, *60*, 5649−5658.
(32) Cai, M.; Mayorov, A. V.; Cabello, C.; Stankova, M.; Trivedi, D.; Hruby, V. J. Novel 3D Pharmacophore of r-MSH/ç-MSH Hybrids Leads to Selective Human MC1R and MC3R Analogues. *J. Med. Chem.* **2005**, *48*, 1839−1848.
(33) Handl, H. L.; Vagner, J.; Yamamura, H. I.; Hruby, V. J.; Gillies, R. J. Lanthanide-based time-resolved fluorescence of in cyto ligand-receptor interactions. *Anal. Biochem.* **2004**, *330*, 242−250.
(34) Yang, Y.; Hruby, V. J.; Chen, M.; Crasto, C.; Cai, M.; Harmon, C. M. Novel Binding Motif of ACTH Analogues at the Melanocortin Receptors. *Biochemistry* **2009**, *48*, 9775−9784.
(35) Liang, L.; Angleson, J. K.; Dores, R. M. Using the human melanocortin-2 receptor as a model for analyzing hormone/receptor interactions between a mammalian MC2 receptor and ACTH(1−24). *Gen. Comp. Endocrinol.* **2013**, *181*, 203−210.
(36) Hruby, V. J.; Cai, M.; Cain, J. P.; Mayorov, A. V.; Dedek, M. M.; Trivedi, D. Design, synthesis and biological evaluation of ligands selective for the melanocortin-3 receptor. *Curr. Top. Med. Chem.* **2007**, *7*, 1107−1119.
(37) Sohn, J. W.; Harris, L. E.; Berglund, E. D.; Liu, T.; Vong, L.; Lowell, B. B.; Balthasar, N.; Williams, K. W.; Elmquist, J. K. Melanocortin 4 receptors reciprocally regulate sympathetic and parasympathetic preganglionic neurons. *Cell* **2013**, *152*, 612−619.
(38) Biebermann, H.; Kuhnen, P.; Kleinau, G.; Krude, H. The neuroendocrine circuitry controlled by POMC, MSH, and AGRP. *Handb. Exp. Pharmacol.* **2012**, 47−75.
(39) Chhajlani, V. Distribution of cDNA for melanocortin receptor subtypes in human tissues. *Biochem. Mol. Biol. Int.* **1996**, *38*, 73−80.
(40) Barkey, N. M.; Tafreshi, N. K.; Josan, J. S.; Silva, C. R. D.; Sill, K. N.; Hruby, V. J.; Gillies, R. J.; Morse, D. L.; Vagner, J. Development of melanoma-targeted polymer micelles by conjugation of an MC1R specific ligand. *J. Med. Chem.* **2011**, *54*, 8078−8084.
(41) Young, S. W.; Qing, F.; Harriman, A.; Sessler, J. L.; Dow, W. C.; Mody, T. D.; Hemmi, G. W.; Hoill, Y.; Miller, R. A. Gadolinium(III) texaphyrin: A tumor selective radiation sensitizer that is detectable by MRI. *Proc. Natl. Acad. Sci. U. S. A.* **1996**, *93*, 6610−6615.
(42) Sessler, J. L.; Miller, R. A. Texaphyrins. New Drugs with Diverse Clinical Applications in Radiation and Photodynamic Therapy. *Biochem. Pharmacol.* **2000**, *59*, 733−739.
(43) Viala, J.; Vanel, D.; Meingan, P.; Lartigau, E.; Carde, P.; Renchler, M. Phases IB and II Multidose Trial of Gadolinium Texaphyrin, a Radiation Sensitizer Detectable at MR Imaging: Preliminary Results in Brain Metastases. *Radiology* **1999**, *212*, 755−759.
(44) Sessler, J. L.; Mody, T. D.; Hemmi, G. W.; Lynch, V.; Young, S. W.; Miller, R. A. Gadolinium(III) texaphyrin: A novel MRI contrast agent. *J. Am. Chem. Soc.* **1993**, *115*, 10368−10369.
(45) Carie, A.; Rios-Doria, J.; Costich, T.; Burke, B.; Slama, R.; Skaff, H.; Sill, K. IT-141, a Polymer Micelle Encapsulating SN-38, Induces Tumor Regression in Multiple Colorectal Cancer Models. *J. Drug Delivery* **2011**, *2011*, No. 869027.
(46) Xu, L.; Josan, J. S.; Vagner, J.; Caplan, M. R.; Hruby, V. J.; Mash, E. A.; Lynch, R. M.; Morse, D. L.; Gillies, R. J. Heterobivalent ligands target cell-surface receptor combinations in vivo. *Proc. Natl. Acad. Sci. U. S. A.* **2012**, *109*, 21295−21300.
(47) Tafreshi, N. K.; Huang, X.; Moberg, V. E.; Barkey, N. M.; Sondak, V. K.; Tian, H.; Morse, D. L.; Vagner, J. Synthesis and characterization of a melanoma-targeted fluorescence imaging probe by conjugation of a melanocortin 1 receptor (MC1R) specific ligand. *Bioconjugate Chem.* **2012**, *23*, 2451−2459.
(48) Sessler, J. L.; Krill, V.; Hoehner, M. C.; Chin, K. O. A.; Davila, R. M. New texaphyrin-type expanded porphyrins. *Pure Appl. Chem.* **1996**, *68*, 1291−1295.
(49) Sessler, J. L.; Mody, T. D.; Hemmi, G. W.; Lynch, V. M. Synthesis and Structural Characterization of lanthanide(III) texaphyrins. *Inorg. Chem.* **1993**, *32*, 3175−3187.
(50) Tafreshi, N. K.; Bui, M. M.; Bishop, K.; Lloyd, M. C.; Enkemann, S. A.; Lopez, A. S.; Abrahams, D.; Carter, B. W.; Vagner, J.; Grobmyer, S. R.; Gillies, R. J.; Morse, D. L. Noninvasive detection of breast cancer lymph node metastasis using carbonic anhydrases IX and XII targeted imaging probes. *Clin. Cancer Res.* **2012**, *18*, 207−219.
(51) Ehrlich, J.; Bogert, M. T. Experiments in the veratrole and quinoxaline groups. *J. Org. Chem.* **1947**, *12* (4), 522−534.